Performance of the deformable mirror for Subaru LGSAO

Shin Oya[a], Aurelien Bouvier[a], Olivier Guyon[a], Makoto Watanabe[a], Yutaka Hayano[a], Hideki Takami[a], Masanori Iye[b], Masayuki Hattori[a], Yoshihiko Saito[a], Meguru Itoh[a], Stephen Colley[a], Mathew Dinkins[a], Michael Eldred[a], Taras Golota[a]

[a]Subaru Telescope, NAOJ, 650 North A'ohoku Place, Hilo, Hawaii 96720, USA;
[b]National Astronomical Observatory of Japan (NAOJ), 2-21-1 Osawa, Mitaka, Tokyo 181-8588, Japan

ABSTRACT

The performance of a deformable mirror with 188 electrodes is reported in this paper. The deformable mirror has been manufactured by CILAS for a new adaptive optics system at Subaru Telescope equipped with laser-guide-star. The type of deformable mirror is bimorph PZT with the blank diameter of 130 mm (beam size 90 mm).

Keywords: adaptive optics system, deformable mirror, bimorph

1. INTRODUCTION

A project updating the adaptive optics (AO) system of Subaru Telescope[1,2] to a laser-guide-star adaptive optics (LGSAO)[3,4] is going on. One of the key components in the system is a deformable mirror (DM). The DM consists of two PZT plates in the configuration of bimorph and has 188 control electrodes in-between. An optical-quality glass plate is glued on the mirror side of the DM and another glass plate on the other side (wiring side) to keep symmetrical structure. Finite element analysis (FEA) had been performed to finalize the specification, by taking account of trade-off between stroke and the size of each electrode, between resonance frequency and the diameter of blank (Ref.5). The DM has been manufactured by CILAS based on the specification. In this paper, the performance of the DM is presented together with comparison between the test results and FEA.

2. SPECIFICATION

Although the most items of the specification had been determined based on a simulation[6] as reported in the the previous work[5], there have been some revisions. A part of them is modified to improve performance and the other part results from the result of manufacturing process. For convenience, the updated specification is summarized in Table 1. The item whose figure has been changed, is indicated by an asterisk in the table. Note that stroke and resonance frequency was not specified because we prefer to specify material and mechanical size of DM based on the FEA result. Comments on some items can be found in the following subsections.

2.1. Electrode Pattern

The electrode pattern is designed as a Voronoi-diagram to gain the stroke of each electrode (Fig.1). The geometrical parameter has been slightly changed before manufacturing for better performance based on an updated result of simulation (Tab.2).

2.2. Reflectivity

An absorption feature is found between 2.7 μm and 3.5 μm (Fig.2). The feature is attributed to adsorption of water vapor in the protect coating layer of the mirror. The maximum depth of the absorption appears at 2.9 μm and increases with the amount of water vapor, from 1.5% in dry nitrogen to 7.5% in wet condition. Although the feature is outside of the L band, a special care on variation of humidity might be necessary in the case of spectroscopic observation around the shorter wavelength edge of the L band.

Further author information: (Send correspondence to S.O.)
S.O.: E-mail: oya@subaru.naoj.org, FAX: 1 808 934 5099

Advances in Adaptive Optics II, edited by Brent L. Ellerbroek, Domenico Bonaccini Calia,
Proc. of SPIE Vol. 6272, 62724S, (2006) · 0277-786X/06/$15 · doi: 10.1117/12.670773

Table 1. Specification of deformable mirror for Subaru LGSAO (Updated)

PZT material		P188
Glass material		BK7
Effective aperture		90 mm
Blank diameter *		130 mm
Thickness *	glass (each side)	< 0.1 mm
	PZT	1.8 mm
Flatness	(wavefront)	30 nm rms
	(incl. mounting err)	< 10% of full stroke range
Hysteresis		< 20% of full stroke range
Surface roughness		<10 Å
Spectral coverage		0.45-6 μm
Coating		protected silver
Reflectivity *	0.45-0.5μm (average)	>95%
	0.5-0.98μm	>97%
	1.0-1.7μm	>97.5%
	1.7-6.0μm *	>99% (except at 2.9μm)
Angle of incidence		16°
Applying voltage		±400 V
Gap between electrodes		<0.7 mm
Operational temperature		$-5 \sim 15$ °C
Altitude		$0 - 4500$ m
Relative humidity		$0 - 90$ %

*: Changed after the previous SPIE meeting (Ref.5).

Table 2. Geometrical parameters of the electrode pattern on the deformable mirror (Revised)

Ring ID Number	Number of electrode	Radius ratio (ring/beam)
1	18	0.335
2	24	0.458
3	30	0.581
4	36	0.704
5	40	0.827
6	40	0.950

The outer edge of the sixth ring is 1.35 × beam radius.

2.3. Hysteresis

A new material type of PZT, P188, is selected for our DM instead of CILAS standard material, P762. The transverse piezoelectric coefficient d_{31} of P188 is 193.5×10^{-12} [m/V] and 1.3 times larger than that of P762. A drawback of P188 is its large hysteresis. The measured hysteresis is 20% for full stroke of ±400 [V]; five times as large as that of P762.

3. TEST RESULTS

3.1. Stroke and vibration properties

The test results on the two major properties of DM: stroke and vibration, are compared with FEA results. After testing the DM, we noticed that the measured properties are well explained without correction for influence of

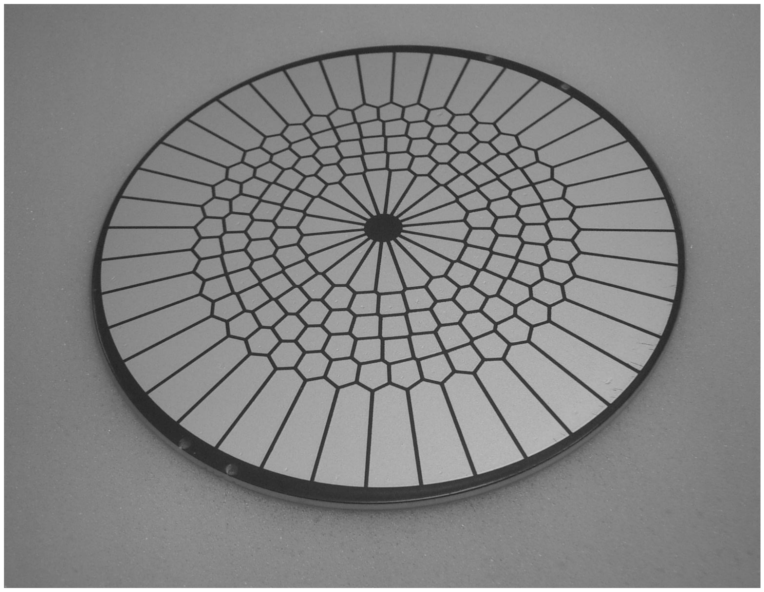

Figure 1. Photograph indicating electrode pattern of the deformable mirror (DM) for Subaru LGSAO.

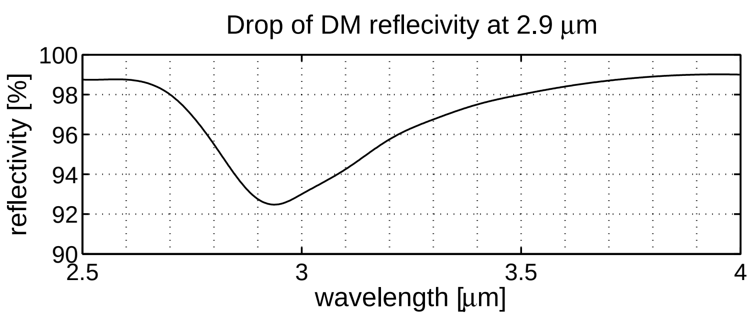

Figure 2. Drop of reflectivity of the deformable mirror (DM). The measurement was done under wet condition.

glass plate on the both surfaces of the bimorph PZT plate. Note that the formula used in Ref.5 is consistent with the experience of CILAS, according to their design report. A possible reason is that the glass plate was polished thinner than the specification to get rid of a defect found during the polishing process.

3.1.1. Stroke

The global curvature R of deformable mirror can be estimated from: applied voltage V, the thickness of one side of bimorph PZT (i.e., a half of the total thickness of bimorph PZT) h, and transverse piezoelectric coefficient d_{31} as

$$R = \frac{h^2}{V d_{31}}, \tag{1}$$

For our DM $h = 0.9 \times 10^{-3}$ [m] and $|d_{31}| = 193.5 \times 10^{-12}$ [m/V], so that $R = 10.5$ [m] when $V = 400$ [V] is applied. The correction factor[5] for influence of the glass plate is 1.45 with these parameters; the curvature corrected for the factor is 15.2 [m]. The measured global curvature of the deformable mirror is 11.2 ± 1.4[m];

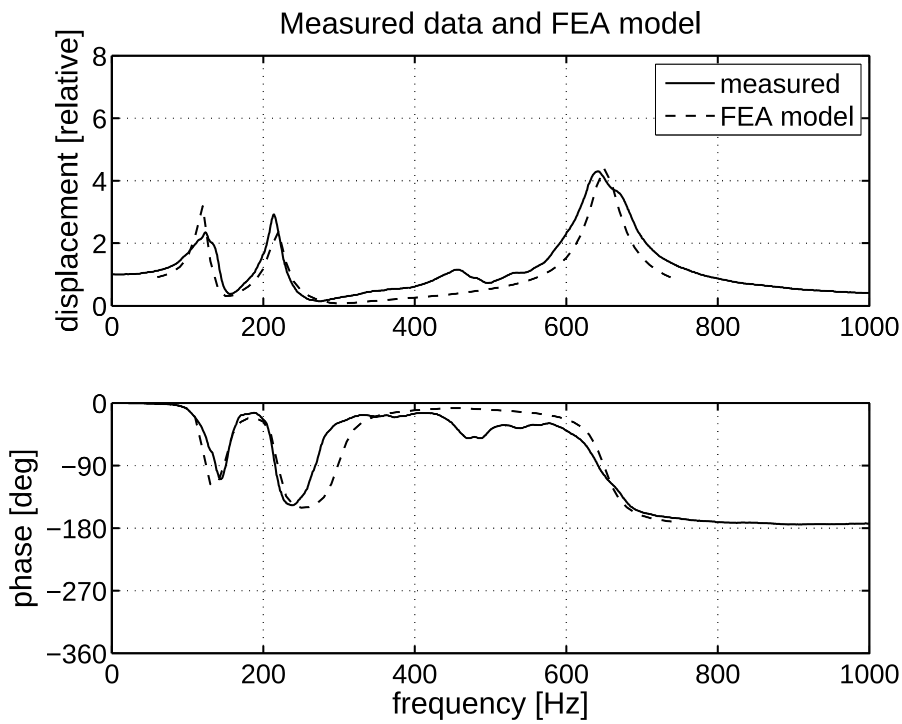

Figure 3. The transfer function of the deformable mirror (DM). The solid line is measured data and the dashed line is a calculated result by an FEA model.

hence, closer to the figure without the glass correction. The situation is the same for the local stroke, except for an electrode in the outermost ring. Measured stroke of the deformable mirror in terms of curvature, is compared with estimation by FEA in Table 3.

Table 3. Measured stroke compared with FEA estimation

EL position	Curvature radius [m]		
	Measured	FEA w/o glass cor.	FEA w/ glass cor.
innermost	14.1	17.9±1.2	26.0±1.7
intermediate	16.0	15.7±0.7	22.8±1.0
outermost	11.0	7.6±2.0	11.0±2.9
global	10.1	11.7	17.0

3.1.2. Vibration

The transfer function in terms of displacement of the mirror surface was measured by applying 1 [V] sinusoidal voltage to all of the electrodes. The data were measured optically by a laser displacement sensor at the center of the DM. A spectrum analyzer was utilized to generate the sinusoidal voltage signal and to record the data synchronized with the applied signal. The measured result is plotted in Figure 3 by solid line.

In addition to the expected peaks around 200 [Hz] and 650 [Hz], there are two more peaks found around 100 [Hz] and 450 [Hz] which are not expected in the previous work[5]. These features can be explained once we take the support structure into account. The DM is supported from the side by three sticks made of PTFE in

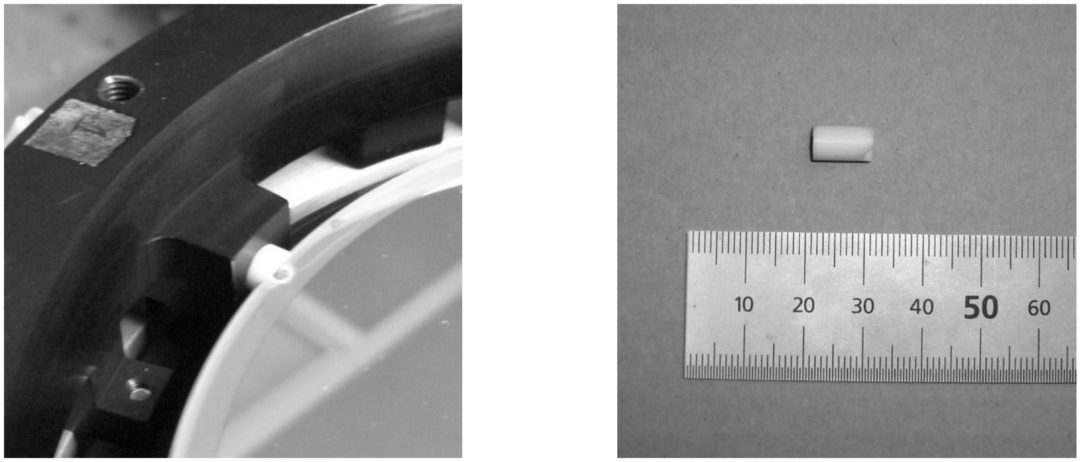

Figure 4. Support structure of the deformable mirror (DM). The left panel shows the structure of a support point and the right panel shows a support stick made of PTFE.

a ring-shape holder made of aluminium. One of the three support-points is shown in the left panel of Figure 4. A hole is drilled on the holder parallel to the mirror surface and in direction toward the center of the DM. The stick (the right panel of Fig.4) is pushed toward the center of the DM in the hole by a set screw. The three support-points are equally separated by 120°. A spring is inserted between the stick end and the screw for one of the three holes to adjust the force applied on the DM.

The support structure of the PTFE stick has been included in the FEA model as a spring with damper. The spring constant and damping constant are parameters required to complete the analysis; however, it is generally difficult to determine these parameters a priori only from the data sheet of PTFE. Therefore, these parameters are determined to reproduce the observed results. First, the spring constant was estimated from Young's modulus of PTFE ($E = 4.8 \times 10^8$ [N/m^2]) and adjusted to fit the modes at the observed frequency (Tab.4). The result of modal analysis does not depend on the damping constant. The adjusted spring constant is smaller by an order

Table 4. Frequency of vibration modes

Mode	Measured [Hz]	FEA calc. [Hz]
1st	124	120
2nd *	214	218
3rd *	457	462
4th	641	648

*: Two modes are degenerated at the frequency.

of magnitude than the initially estimated value. This is probably because the PTFE stick is not fixed rigidly enough as it is in the FEA model. The shapes of modes are displayed in Figure 5. The upper-left panel shows the first mode at 121 [Hz]. The shape of the mode is piston-like; the upper-right, the second-mode at 219 [Hz] (tilt superimposed with slight trifid components); the middle-left, the third-mode at 462 [Hz] (astigmatism-like); the middle-right, the fourth-mode at 648 [Hz] (defocus-like). The next step is to determine the damping constant to fit the width of peak of the amplitude in the transfer function. During this step, we found that perfectly symmetric model does not show the peaks corresponding degenerated modes at 219 [Hz] and 462 [Hz] in the amplitude of the calculated transfer function. Asymmetry introduced by applying downward force on back side as a boundary condition is successful to reproduce the observed peaks. It might be caused by pins and wires on the back side of the DM. The calculated transfer function by FEA is plotted in Figure 3 by dashed line. In order

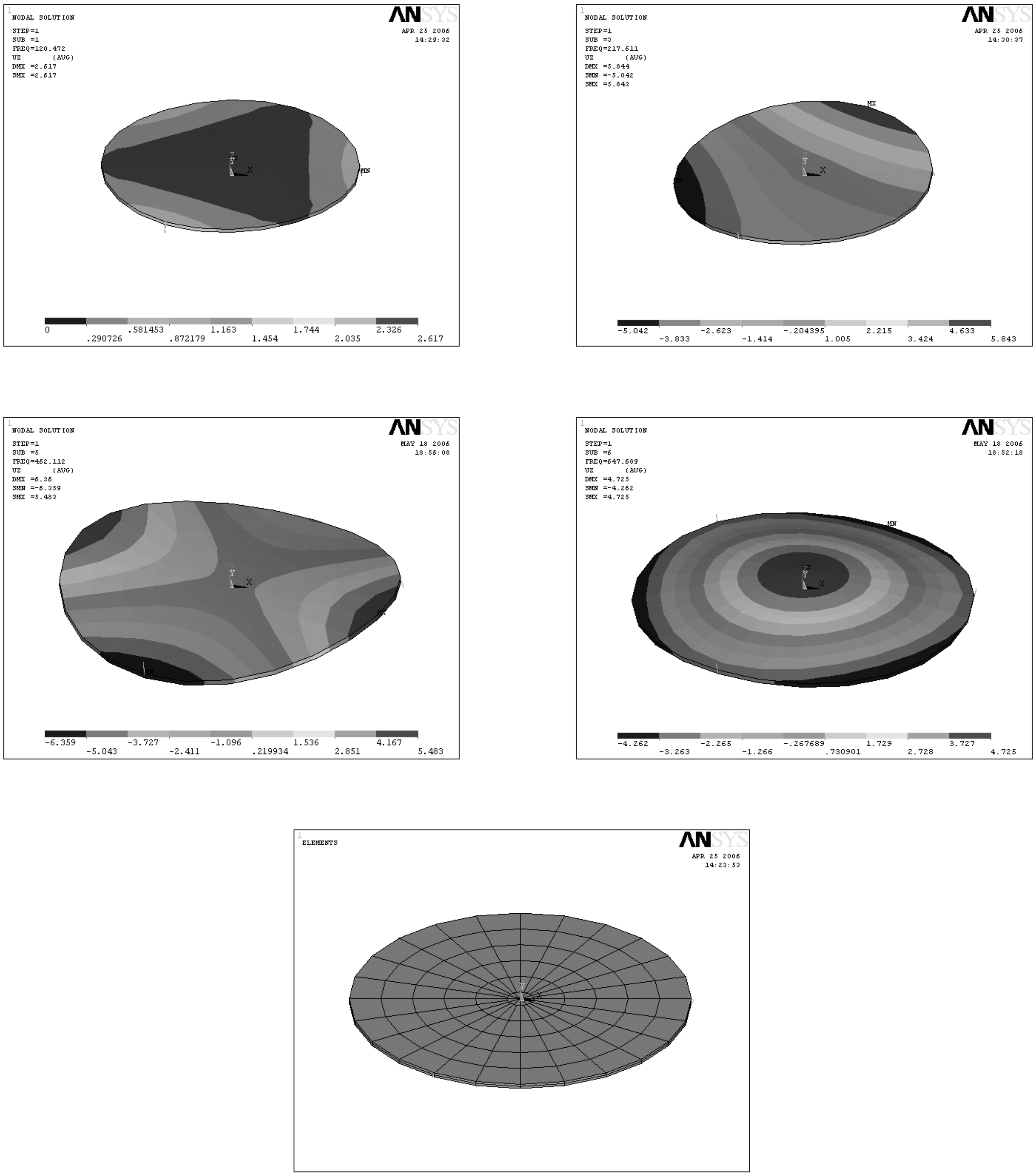

Figure 5. Results of modal analysis and the model use by FEA for the deformable mirror with the support structure

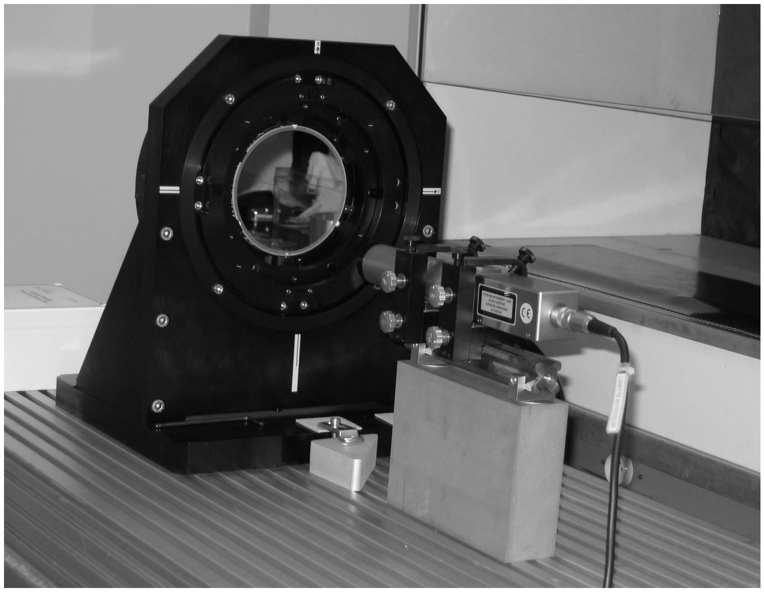

Figure 6. The deformable mirror held in the tip/tilt-mount

to repeat the process quickly, a simplified model with 438 nodes are used as shown in the lower panel of Figure5. As a result, correction of glass plate is not necessary to fit the experimental data neither from the point of view of dynamic properties in the FEA model.

3.2. Tip/tilt mount

The basic structure of the DM holder and mount follows the design of that for MACAO-VLT.[7] The ring-shape DM holder is mounted in a tip/tilt mount (TTM) on the AO optics bench.[8] The suppression of the artificial thermal background pattern[2] observed during dithering by nodding TTM, is expected by this configuration. The TTM has been designed and fabricated by Observatoire de Paris. The center of the gravity of the DM and the holder is designed to be the same point as the center of the DM optical surface and the center of the motion of TTM. As a result of fitting test (Fig.6), the difference of balance between with and without DM measured by capacitance sensor of TTM was quite small (less than 1% of full stroke of the TTM). We also confirmed that the vibration was well isolated between DM and TTM. The transfer functions with and without DM were obtained, electrically by the TTM capacitance sensor and optically by autocollimator (a small piece of flat mirror was attached for the optical measurement without DM); The result of comparison did not show any clear difference.

4. FUTURE WORK

An FEA model of the DM has been updated to reproduce the test results of the dynamic performance better. The possible next step will be to find a mechanical design to improve the transfer function based on the FEA model.

5. SUMMARY

The deformable mirror (DM) for laser-guide-star adaptive optics (LGSAO) of Subaru Telescope has been fabricated. Performance of DM was tested and found to be satisfactory. Regarding two important properties of DM: stroke and vibration, the measured data were compared with FEA calculations. These results will be helpful to improve performance of DM in future.

ACKNOWLEDGMENTS

We wish to express our gratitude to Jean-Christophe Sinquin who helped us a lot about the design and manufacturing of the deformable mirror as a project manager of CILAS. Jean-Marie Lurcon and Claude Guillemard supported us at the acceptance test. We are grateful to Pierre Gigan of Observatoire de Parise for his considerate help toward the test of DM with the tip/tilt mount.

REFERENCES

1. H. Takami, N. Takato, Y. Hayano, M. Iye, S. Oya, Y. Kamata, T. Kanzawa, Y. Minowa, M. Otsubo, K. Nakashima, W. Gaessler, and D. Saint-Jacques, "Performance of Subaru Cassegrain Adaptive Optics System," *Publ. Astron. Soc. Japan* **56**, pp. 225–234, 2004.
2. S. Oya, N. Takato, H. Takami, Y. Hayano, M. Iye, H. Terada, K. Murakawa, Y. Minowa, M. Hattori, M. Watanabe, Y. Kamata, T. Kanzawa, T. Kane, and W. Gaessler, "Subaru adaptive optics system after two years of open use," in *Advancements in Adaptive Optics*, D. Bonaccini, B. L. Ellerbroek, and R. Ragazzoni, eds., *Proc. SPIE* **5490**, pp. 409–420, 2005.
3. H. Takami, M. Iye, Y. Hayano, Y. Saito, Y. Kamata, N. Arimoto, N. Takato, S. Colly, M. Eldred, T. Kane, O. Guyon, S. Oya, M. Watanabe, M. Hattori, M. Goto, N. Kobayashi, and Y. Minowa, "Laser guide star AO project at the Subaru Telescope," in *Advancements in Adaptive Optics*, D. Bonaccini, B. L. Ellerbroek, and R. Ragazzoni, eds., *Proc. SPIE* **5490**, pp. 837–845, 2004.
4. H. Takami, S. Colly, M. Dinkins, M. Eldred, G. Taras, O. Guyon, M. Hattori, Y. Hayano, M. Itoh, M. Iye, S. Oya, Y. Saito, and M. Watanabe, "Status of Subaru laser guide star AO system," in *Advance in Adaptive Optics II*, B. L. Ellerbroek and D. Bonaccini, eds., *Proc. SPIE* **6272**, 2006. Code Number [6272-12].
5. S. Oya, O. Guyon, M. Watanabe, Y. Hayano, H. Takami, M. Iye, N. Arimoto, S. Colly, M. Eldred, T. Kane, M. Hattori, Y. Saito, Y. Kamata, N. Kobayashi, Y. Minowa, M. Goto, and N. Takato, "Deformable mirror design of Subaru LGSAO system," in *Advancements in Adaptive Optics*, D. Bonaccini, B. L. Ellerbroek, and R. Ragazzoni, eds., *Proc. SPIE* **5490**, pp. 1546–1555, 2004.
6. O. Guyon, N. Arimoto, C. Blain, S. Colly, M. Eldred, M. Goto, M. Hattori, Y. Hayano, M. Iye, Y. Kamata, T. Kane, N. Kobayashi, M. Watanabe, Y. Minowa, S. Oya, Y. Saito, H. Takami, and N. Takato, "Subaru Telescope LGSAO: overview of expected performance," in *Advancements in Adaptive Optics*, D. Bonaccini, B. L. Ellerbroek, and R. Ragazzoni, eds., *Proc. SPIE* **5490**, pp. 733–741, 2004.
7. R. Arsenault, J. Alonso, H. Bonnet, J. Brynnel, B.Delabre, R. Donaldson, C. Dupuy, E. Fedrigo, J. Farinato, N. Hubin, L. Ivanescu, M. Kasper, J. Paufique, S. Rossi, S. Tordo, S. Stroebele, J. L. Lizon, P. Gigan, F. Delplancke, A. Silber, M. Quattri, and R. Reiss, "MACAO-VLTI: An Adaptive Optics System for the ESO Interferometer," in *Adaptive Optical System Technologies II*, P. L. Wizinowich and D. Bonaccini, eds., *Proc. SPIE* **4839**, pp. 174–185, 2003.
8. M. Watanabe, H. Takami, N. Takato, S. Colly, M. Eldred, T. Kane, O. Guyon, M. Hattori, M. Goto, M. Iye, Y. Hayano, Y. Kamata, N. Arimoto, N. Kobayashi, and Y. Minowa, "Design of the Subaru laser guide star adaptive optics module," in *Advancements in Adaptive Optics*, D. Bonaccini, B. L. Ellerbroek, and R. Ragazzoni, eds., *Proc. SPIE* **5490**, pp. 1096–1104, 2004.